J Mater Sci (2012) 47:583–598
DOI 10.1007/s10853-011-5995-5

ANNIVERSARY REVIEW

Wood: A 45th anniversary review of JMS papers

Part 2. Wood modification, fire resistance, carbonization, wood–cement and wood–polymer composites

Martin P. Ansell

Received: 25 August 2011 / Accepted: 23 September 2011 / Published online: 12 October 2011

Abstract The second part of a comprehensive review of the literature on wood published in the *Journal of Materials Science* since its inception in 1966 is presented. The topics reviewed include wood modification and surface treatment, the thermal stability of wood and resistance to fire, the physical properties of wood chars and wood-based carbon materials, and the structure-related properties of wood–cement and wood–polymer composites. The articles reflect the wide range of techniques utilised to improve wood properties, the role of wood as a precursor for carbon-based materials and cellular ceramics and the application of wood as a composite reinforcement. JMS is in the vanguard of the latest developments in all these disciplines.

Introduction

In Part 1 of this JMS review [1], the properties of the wood cell wall were examined and the key role of the cellulose microfibril angle (MFA) and moisture content in determining wood properties was explained. The effects of moisture, time and temperature on the creep and stress relaxation of wood were reviewed, and the mechanical properties of wood including fracture and fatigue were evaluated. The articles in Part 1 reflected a global interest in wood as a structural material with an expanding output of research material in JMS. Part 2 is concerned with the protection of wood from the adverse effects of moisture and fire by modification, ingenious techniques for the production of carbon-based materials and porous ceramics for technical applications and methods for manufacture or synthesis of cement and polymer matrix composites and the measurement of their physical properties.

Wood modification is a field of intense activity which has recently been reviewed by Hill in a seminal textbook [2]. The subject includes the protection of wood from biodegradation (fungal and insect attack) and weathering using chemical or thermal treatments. JMS articles include research on acetylation which is a commercial process for the treatment of timber, where reaction of acetic anhydride with the wood cell wall converts polymeric hydroxyl groups into acetyl groups with the formation of an ester bond. Following treatment, moisture uptake is significantly reduced, and the wood becomes indigestible to insects. Furthermore, the process is non-toxic, and wood surfaces become more compatible with paints and varnishes. Other modification processes described in the pages of JMS include enzymatic modification and treatment of wood with boron and oil. The review also examines changes in the surface chemistry and density of wood following densification and ultrasonic cutting.

Thermal modification is a process whereby wood is treated in an inert gas atmosphere at temperatures up to 260 °C, resulting in the shrinkage of the wood accompanied by an increase in elastic modulus and some embrittlement. The high temperature destroys fungal bodies in cell cavities, decay is inhibited and dimensional stability is improved. New developments in the protection of wood from combustion by fire include the incorporation of silicones into the cellular structure of wood and impregnation with salts by reaction with supercritical carbon dioxide (sc-CO_2). The deposition of thin titania films on the surface of wood using a cosolvent-controlled hydrothermal technique is another state-of-the-art technique for fire protection.

M. P. Ansell (✉)
Department of Mechanical Engineering, BRE Centre for Innovative Construction Materials, University of Bath, Bath BA2 7AY, UK
e-mail: M.P.Ansell@bath.ac.uk

Carbonised wood in the form of charcoal was a key ingredient of the industrial revolution, used in foundries for the smelting of iron. It now finds applications in a wide range of technologies for the production of electrodes, control of pollution, dissipation of heat and gas storage. Charcoal maintains the structural geometry of the original wood, and it may act as a matrix for infiltrated metal alloys or ceramic phases. Alternatively, carbonised wood may be infiltrated by ceramic constituents which remain when the carbon template has been burnt away by pyrolysis.

In the construction industry there are currently strong incentives to increase sustainability, reduce weight and improve thermal properties, and wood-based composites contribute to making improvements in the environmental performance of materials. Wood–cement composites in the form of particleboard or plasterboard have contributed to the reduction in the energy-intensive production of cement and a commensurate reduction in carbon dioxide emissions. Wet strength, dimensional stability and optimum conditions for hydration are factors which are considered in this review. Wood–polymer composites (WPCs) are familiar in the form of plywood, chipboard, medium-density fibreboard (MDF) and oriented strandboard (OSB) for timber frame construction and decking. JMS has been in the forefront of disseminating new advances in this field. Synthetic and natural (e.g. tannins and starches) thermoplastic and thermosetting polymer matrix composites are described with emphasis on utilising wood wastes and optimising physical properties.

As in Part 1 of this article, references are largely restricted to JMS publications but additional key references are included where appropriate. The references quoted at the end of each JMS article provide the reader with a very comprehensive view of the wider literature.

Wood modification

The effect of chemical treatments on the dynamic mechanical properties of Sitka spruce (*Picea sitchensis* Carr.) heartwood was examined by Sugiyama et al. [3]. The four treatments employed were formaldehyde modification (formalisation), acetylation, propylene oxide (PO) treatment with a triethylamine (TEA) catalyst and polyethylene glycol (PEG) impregnation in an aqueous solution. All four treatments were said to be relatively benign, modifying the amorphous components of the wood rather than the crystalline cellulose. The dynamic viscoelastic properties of the spruce wood were measured to assess changes in the mechanical response of the wood cell wall, and a simple model was proposed to predict the storage (E') and loss (E'') moduli and loss tangent (tan δ) of the modified wood. Viscoelastic properties were measured using a dynamic viscoelastometer and fitted to the model to predict specific gravity and the volume fraction of microfibrils in the wood cell wall. Formaldehyde treatment resulted in the formation of oxymethylene linkages between hydroxyl groups which markedly increased dimensional instability. A reduced tan δ above 100 °C was said to be associated with restricted micro-Brownian movement in the amorphous component of the wood cell wall. Acetylation introduced bulky acetyl groups which reduced cohesion between matrix polymer chains causing plasticisation and reduced dynamic modulus. PO treatment substituted bulky OCH_2-$CH(OH)C_2H_5$ groups in place of OH groups, again causing plasticisation and increased tan δ above 100 °C. Finally, PEG bulked up the wood cell wall and also acted as a plasticiser, reducing the dynamic elastic modulus and increasing damping above −50 °C.

In a related study on the dielectric properties of Sitka spruce (*Picea sitchensis* Carr.) heartwood, Sugiyama and Norimoto [4] extracted and air-dried spruce specimens and subjected them to the four treatments discussed above [3]. In addition, the spruce was treated with phenol formaldehyde (PF) resin and wood methyl methacrylate (MMA), and the final treatment involved thermal modification in a vacuum oven at 180 °C. The dielectric constant (ε') and dielectric loss (ε'') were measured along the grain over 31 steps of frequency from 1 kHz to 1 MHz in the temperature range from −150 to 20 °C for untreated wood and following the seven chemical and thermal treatments. Contour maps of ε' and ε'' were generated in plots of temperature versus log frequency. The Cole–Cole circular arc law was applied to the data for dielectric relaxation, and relaxation spectra were derived, each with a generalised relaxation time. Amongst the results reported, PEG treatment caused the highest weight percent gain (178.6%) resulting in the highest peak value in the relaxation spectrum with the narrowest distribution of relaxation times. The reverse was observed for acetylation where weight gain following treatment was 25.8% resulting in the lowest peak value in the relaxation spectrum with the widest distribution of relaxation times. Relaxation behaviour was attributed to the motion of methylol groups associated with each chemical or thermal treatment.

The swelling of acetylated wood by organic solvents was considered by Obataya and Shibutani [5] to reduce the dimensional stability of WPCs. Various organic liquids act as diluents for recycled polymers which could be incorporated into wood cell walls following acetylation to facilitate the manufacture of dimensionally stable acetylated WPCs. The sapwood of ezomatsu (*Picea yezoensis*) was acetylated resulting in a 21.1% weight gain and 6.9% increase in volume. Untreated and acetylated wood was soaked in a wide range of organic liquids, and volumetric swelling was measured. Little or no swelling of untreated

wood immersed in aromatic and aliphatic non-polar liquids was observed because these liquids possess weak hydrogen bonds and are unable to penetrate the hydrophilic wood polymers which contain strong intermolecular bonds. In contrast, acetylated wood was heavily swollen by aromatic liquids following acetylation because hydroxyl groups have been replaced by bulky acetyl groups, and there are fewer intermolecular hydrogen bonds in the modified wood. However, the polar nature of the acetyl groups interfered with the access of the molecules of aliphatic liquids resulting in little change in volume.

A fourth article from Japan [6] examined the change in properties of Yezo spruce (*Picea jezoensis* Carr.) following treatment with an aqueous amine solution (ethylenediamine, EDA) which is capable of penetrating native crystalline cellulose in the wood cell wall. Swelling plasticises the wood, and the process can be used for the manufacture of bent wood products. The spruce was treated with a range of aqueous concentrations of EDA, and at a concentration greater than 70%, a reduction in the elastic modulus as measured in 3-point bending was observed, corresponding with the conversion of cellulose I to cellulose III_I as measured by X-ray diffraction (XRD). Increasing relative humidity further reduced the elastic modulus.

The enhancement of the deformability of the wood cell wall was also investigated by Goswami et al. [7]. They employed enzymatic modification with the motive of increasing the flexibility of wood veneers used in the automotive industry. Spruce wood fibres (*Picea abies* [L.] Karst.) were extracted from microtomed sections and treated with the enzyme 'Cellulase Onozuka R-10 from *Trichoderma viride* (E.C.3.2.1.4)' constituents of which are known to break down the main backbone and end chains of cellulose. Micromechanical tests revealed that the strength and stiffness of enzyme-treated fibres were reduced and that in most cases failure was brittle. However, 20% of the fibre tests resulted in high ductility, and it was proposed that cellulose microfibrils become detached from the lignin/hemicellulose matrix allowing fibrillar glide to occur. FTIR results indicated some minor changes in the intensity of absorption maxima indicating only small chemical changes to the constituents of the cell wall.

A study of the wettability of MDF panels following the thermal modification of constituent fibres at 150 and 180 °C [8] demonstrated that contact angles were increased, and less water was absorbed compared with control panels. The MDF panels were manufactured in the laboratory from 90% softwood fibres, composed of black spruce (*Picea mariana* (Mill.) BPS), balsam fir (*Abies balsamea* (L.) Mill.) and jack pine (*Pinus banksiana* Lamb.), and 10% white birch (*Betula papyrifera* Marshall) fibres. Wettability was measured using the Wilhelmy plate method, illustrated in Fig. 1 with a schematic output presented in Fig. 2. X-ray photoelectron spectroscopy (XPS) allowed the identification of functional groups and the elemental composition of the thermally modified fibres. Depending on the heat-treatment temperature and time, the receding contact angles increased in the range from 41.9 to 53.6° and the advancing contact angle increased by between 5.7 and 14.6°, so that the panels are less hydrophilic following thermal modification. Instant absorption of water by capillary action (wicking) and water absorption following soaking were reduced following thermal treatment of fibres. Only slight modification of surface composition was revealed by XPS analysis with a small decrease in O/C ratio.

Two articles [9, 10] considered methods for reducing the leaching of boron from beech (*Fagus orientalis*) and Scots pine (*Pinus sylvestris*) wood by treatment of the wood with hot vegetable oils. Boron compounds, e.g. boric acid and sodium borate (borax), are an attractive option for the preservation of wood as they are inexpensive, non-toxic, colourless, odourless and non-corrosive. In outdoor applications, boron compounds are readily leached from wood, so that the strategy of treating wood with hydrophobic vegetable oils is attractive. In the first article [9], leaching tests were performed on boron impregnated wood following oil heat treatment. Boron content analysis before and after leaching was performed by Inductively Coupled Plasma Analysis, and promising treatments were analysed thermogravimetrically. The Scots pine retained a high proportion of the boron and oil as a result of its high permeability compared with beech. Waste oil and sunflower oil treatments resulted in the greatest retention of boron. Thermogravimetric analysis (TGA) gave similar results for all treatments, but increased boron content produced more residues. In the second article [10], the same wood species were treated with hot oils as before, and water absorption, efficiency of water repulsion, compressive strength parallel to the grain, colour change and decay resistance were evaluated. Scots pine specimens, on vermiculite mixed with malt extract agar, were inoculated with brown rot fungus *Coniophora puteana* and beech specimens, also on vermiculite mixed with malt extract agar, with the white rot fungus *Coriolus versicolor* and mass loss measured after 60 days. Oil treatment reduced water absorption and improved water repulsion, but the beech treatment was less effective as less oil was absorbed. Compressive strength was little changed following boron treatment at 1, 2 and 5% levels, but colour changes could be problematic with darkening of the wood occurring in some cases. In the decay tests, both unleached and leached specimens were exposed, and the leached specimens suffered the greatest weight loss as expected. Double treatment with 5% boric acid and hot vegetable oils resulted in very small weight losses, and a synergetic effect was proposed.

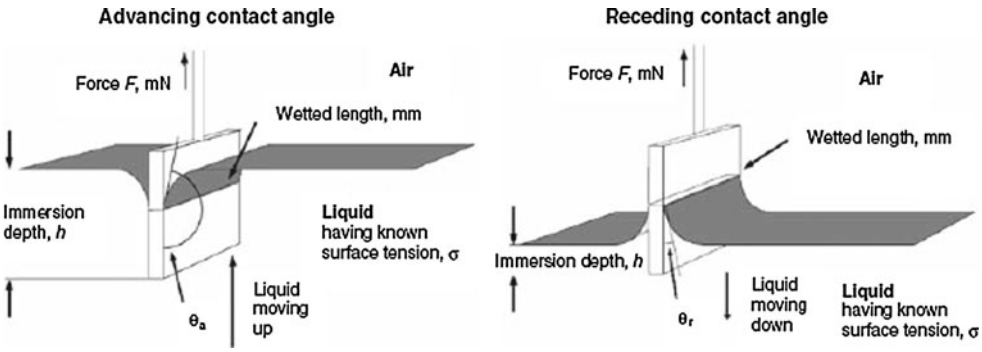

Fig. 1 Immersion in and withdrawal from a liquid to allow advancing and receding contact angle measurements using the Wilhelmy plate method [8]

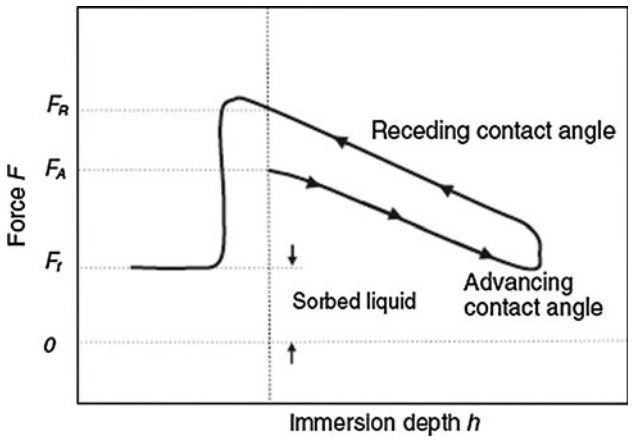

Fig. 2 Schematic of force F versus immersion depth h for Wilhelmy plate test. Forces F_A and F_R are obtained from the advancing and receding curves, respectively, and the final force F_f corresponds to the mass of absorbed liquid [8]

Surface properties of wood

The mechanical deformation of wood surfaces by microtoming and sanding [11], ultrasonic-assisted cutting [12] and densification [13] are considered in this section. In the first [11] of two articles by Sinn and co-workers, XPS was employed to perform a surface analysis of spruce (*Picea abies* Karst.), larch (*Larix decidua* Mill.), beech (*Fagus sylvatica*) and oak (*Quercus robur*) cut with a sledge microtome and sanded with a random orbit sander. The aim was to determine surface chemical changes by measuring the atomic concentration of oxygen to carbon. The microtomed sections possessed higher ratios of oxygen to carbon for all wood species, and scanning electron microscope (SEM) images revealed anatomical features of wood structure which were absent from the sanded wood. An analysis of the C1s peak of the XPS spectrum by deconvolution revealed that the contributions to the peak intensity from cellulose were suppressed following sanding and wood density affected the oxygen to carbon ratio. Lignin-rich and carbon contaminants were increased by ductile deformation in the sanding process and extractives content, high in oak and larch, also influenced surface chemistry. Disappointingly, no study on wettability or surface adhesion was reported.

In the second article [12] the surface properties of Norway spruce (*Picea abies* (L.) Karst.), beech (*Fagus sylvatica* L.) and MDF were examined following conventional cutting and ultrasonically assisted cutting. The wood was cut along the grain (LR plane) in the same mode as a chisel with wedge angle of 45° and a clearance angle of 10°. In ultrasonic mode, longitudinal vibrations were imposed at a frequency of approximately 20 kHz and vibration amplitude of 8 μm. The cut surfaces were inspected by SEM and surface roughness measured with a stylus system. Wettability was assessed in contact angle measurements with water droplets and surface energy was assessed using the acid–base approach. The topography of the conventionally and ultrasonically cut surfaces were similar, but periodic impact marks were clearly visible in the latter case (Fig. 3) for the solid wood. The mean surface roughness of the wood and MDF was also similar, and the wettability of beech was unchanged. The high frequency associated with ultrasonic cutting appears to generate heat which accelerates ageing of the beech wood surface evaluated by changes in surface energy.

Rautkari et al. [13] densified the clear sapwood of Scots pine (*Pinus sylvestris* L.) in a series of experiments designed to assess surface modification as a function of press temperature, closing time, holding time, moisture content and compression ratio. Pressure was applied normal to the grain direction and through thickness density was determined using a density profilometer with a gamma ray source. The earlywood zones near the pine wood surface were the first to be compressed, revealed by SEM examination. Wood softening occurred at lower temperatures for high moisture content, but for long contact times, a reduction in moisture content influenced the density profile. Shorter closing times produced preferred deformation close to the surface, and higher temperatures produced a broader density peak further away from the surface. Overall, the density profile was influenced by the combination of pressing parameters.

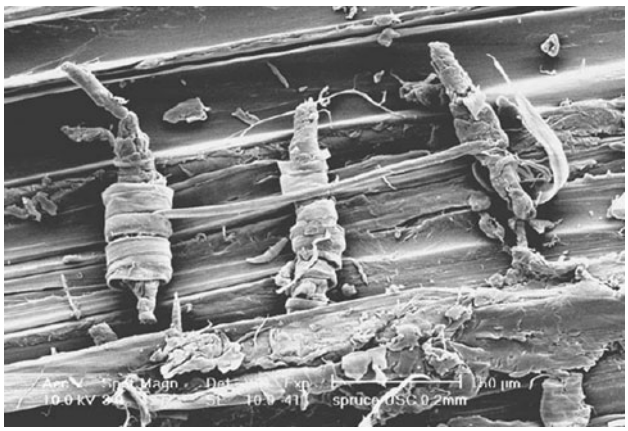

Fig. 3 Reels of spruce wood fibre 10–20 μm in diameter formed by ultrasonic cutting [12]

Thermal modification of wood and resistance to fire

The thermal modification (heat treatment) of wood to enhance mechanical properties and reduce susceptibility to fungal attack is a commercial process (e.g. ThermoWood®) which takes place in an inert gas atmosphere or under a steam blanket well above the temperature used to kiln dry wood in air (up to ~120 °C). Initially. free water in the cell cavity is reduced by drying until it is all removed and the fibre saturation point is reached. At elevated temperatures, the bound water in the cell wall is removed; chemical changes occur to the cellulose, hemicellulose and lignin in the cell wall which collapses causing shrinkage and a reduction in density. Thermally modified wood is specified for external use for applications such as cladding and decking.

Kocaefe et al. [14] heat treated aspen (*Populus* sp.) in a thermogravimetric analyser in a nitrogen atmosphere. The wood was heated to 210, 220 and 230 °C at different rates (10, 20, and 30 °C h^{-1}) and held for times of 0, 15, 30 and 45 min at three gas humidities (0, 80, and 160 g water m^{-3}). Brinell hardness was measured with a steel ball indenter on the radial and tangential faces and flexural strength and stiffness measured in three-point bending. Weight loss (~20%) was the greatest at the highest heating rate, at the highest maximum temperature and for the longest holding time. Following initial moisture loss and evaporation of volatiles, major structural changes took place at 160 °C. The tangential hardness was increased by increasing the heating rate and holding time, and flexural modulus was slightly increased by the level of gas humidity and maximum temperature of treatment. The same research group performed a similar study [15] on North American jack pine (*Pinus banksiana*) where the optimum thermal treatment was sought which maximised bending strength, hardness, screw withdrawal strength and dimensional stability. TGA took place in a nitrogen and carbon dioxide atmosphere under similar conditions reported for the study on poplar [14]. Whilst the dimensional stability of the pine improved following thermal modification, the mechanical properties and screw withdrawal strength generally reduced after treatment above 200 °C. The thermogravimetric approach allows optimum heat treatment parameters for wood to be deduced, whilst providing information on weight changes as a function of temperature, time and the gas environment.

Wood is well known to be flammable in thin sections but, in section thicknesses of 12 cm and above, it produces a char layer which provides protection to beams in severe fires. Surface treatments for wood are available which incorporate inorganic compounds into the cellular structure of wood, often based on titanium and silicon dioxides. Advances in fire protection appear in the pages of JMS, and there is current interest in protective systems based on innovative coating and impregnation techniques. A fascinating article [16] on the flame retardancy of paulownia hardwood (*Pauloumia tomentosa*) compares its performance in fire with cedar softwood (*Cryptomeria japonica*). Unusually, paulownia is known to be naturally flame retardant and has been traditionally used for wardrobes for protecting kimonos from fire in Japan. Paulownia and cedar wood boards were dried to constant weight and heated on an aluminium surface to 450 °C. Time versus weight curves are presented in Fig. 4. After a minute, a 5-mm-thick carbonised layer appeared on the surface of the paulownia whereas only a 1-mm-thick layer formed on the cedar. The carbonised layer has a lower thermal conductivity than wood providing thermal protection. The cedar subsequently developed an ash layer, and the board was consumed after 30 min, but the paulownia produced little ash and survived. The difference is the result of paulownia's thin-walled cellular hardwood structure which has a higher thermal diffusivity than cedar and easily carbonises. The denser cedar softwood also contains more lignin which produces alkanes when heated, as determined by gas chromatography, and is easily combusted. The combustion process was elegantly modelled using finite element analysis (FEA), and models constructed from corrugated article which simulate the structure of paulownia and cedar were employed to demonstrate how microstructure inhibits burning.

A technique for incorporating silicones into aspen wood (*Populus* sp.) which crosslinks the silicones in situ is described by Eastman et al. [17]. The transport and reaction medium for the silicones is sc-CO_2 which is a non-toxic and recoverable solvent. Essentially, the aspen wood is treated with a continuous sc-CO_2 extraction with ethanol as co-solvent and inorganic impurities and free lignin are removed. The aspen wood was immersed in two silicone

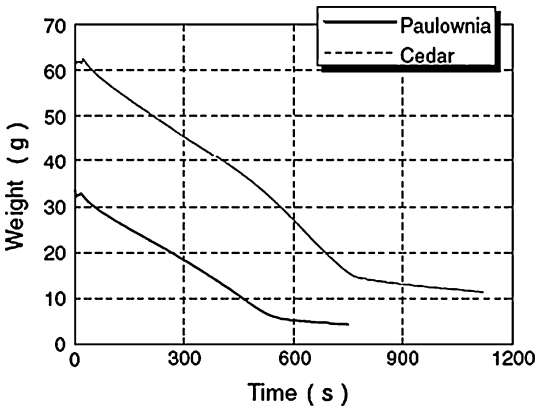

Fig. 4 Time-weight curves for Paulownia and cedar at 50 kW m^{-2} of heat flux [16]

mixtures in a pressurised vessel at 70 °C and a platinum catalyst was introduced after depressurisation and cooling to RT. Hydrosilation crosslinking was achieved by the introduction of pure oxygen, and subsequently the vessel was pressurised with CO_2 at 70 °C to complete the reaction. The fire resistance of the aspen–silicone composite, measured with a pyrolysis combustion flow calorimeter, was significantly improved, and a silicon dioxide glass char was formed as a product of combustion which is thought to act as a protective insulating layer. Mechanical degradation kinetics were followed in a muffle furnace containing an aspen specimen subjected to three-point bending under constant load and an improvement in residual mechanical properties was measured following silicone impregnation.

A second article [18] also employed sc-CO_2 to impregnate spruce (*Picea abies*) and beech (*Fagus* sp.) with water-soluble and water-insoluble salts for the purpose of fire retardation. Wood is immersed in a solution of calcium chloride which is absorbed into the wood structure. Following immersion in sodium hydroxide, calcium hydroxide is precipitated. The impregnated wood is reacted with sc-CO_2 in a high pressure autoclave forming precipitated (prec) calcium carbonate. These reactions are summarised in Eqs. 1 and 2:

$$CaCl_2 + 2NaOH \rightarrow Ca(OH)_{2(prec)} + 2NaCl \quad (1)$$

$$Ca(OH)_{2(prec)} + scCO_2 \rightarrow CaCO_{3(prec)} + H_2O \quad (2)$$

The wood was immersed in 7% w/v PMMA solution in chloroform or 7% silane–siloxane in white spirit to produce a polymer coating which can provide additional fire retardation. The uncoated and coated wood and untreated control samples were assessed by TGA and also subjected to combustion. TGA results demonstrated significant reduction in rate of mass loss following treatment and fire retardation in treated wood was very good.

In a final article on fire retardation, Sun et al. [19] grew thin titanium dioxide coatings on the surface of birch wood (*Betula albosinensis* Burk) using a cosolvent controlled hydrothermal technique. Wood specimens were immersed in an alcoholic solution of tetrabutyl orthotitanate and heated in a sealed reactor at 130 °C for 8 h followed by reaction with sodium dodecyl sulphate for 4 h at 70 °C. The surface composition was assessed by X-ray analysis (EDAX) in a SEM, and chemical functional groups were identified by Fourier Transform Infrared spectroscopy (FTIR). XRD determined the crystalline phase of TiO_2, and combustion testing was performed using a cone calorimeter. SEM revealed evenly grown spheres of TiO_2 on the surface of the treated wood, 300–600 nm in diameter. EDAX, FTIR and XRD confirmed the presence of anatase TiO_2 bonded to the wood hydrocarbons. The combustion time for the treated wood was twice as long as that for untreated wood. Smoke emission was suppressed, and carbon monoxide yields were also reduced in treated wood.

Carbonised wood

The JMS literature on carbonisation of wood is remarkably extensive and covers the production of biomass chars for iron making, the use of activated carbons for pollution control, gas separation and storage, the manufacture of wood ceramics, the conversion of charcoal into ferromagnetic carbon electrodes, the synthesis of carbon fibres, the study of soot from wood combustion and the fabrication and properties of carbon/aluminium and carbon/ceramic composites. The cellular structure of wood allows porous forms of carbon to be produced which may in turn be infiltrated by a second phase enabling a plethora of carbon-based or composite structures to be produced.

In a series of three articles, Kumar and co-workers [20–22] evaluated the physical properties of wood chars manufactured from *Acacia* and *Eucalyptus* wood. They used [20] a muffle furnace to carbonise small cubes of wood ($\sim$1 cm^3) by slow heating to temperatures of 400, 600, 800, 1,000 and 1,200 °C at 4 °C min^{-1} and thermally soaked the carbonised wood for 1 h before slow cooling in the furnace. Soaking time was increased from 1 to 5 h at 800 and 1,000 °C. Rapidly heated wood cubes were placed directly in the furnace at 400, 600, 800 or 1,050 °C, soaked for 1 h and cooled in air. A two-probe technique was employed to measure resistivity using a digital multi-meter or potentiometer. Edge dimensions of carbonised cubes were 0.76–0.78 cm, and the copper electrodes used were 11-mm diameter discs with silver foils between electrode and wood char cube to eliminate contact resistance. The highest carbonisation temperatures resulted in the lowest resistivities, and above 800 °C, the wood species had negligible effect on resistivity. For a soaking time of 1 h above 1,000 °C, the resistivity settled down to between

0.14 and 0.38 Ω cm for slow and rapid heating strategies. It was concluded that electrical resistivity is a good measure of wood char quality. XRD enabled the crystalline structure of the wood chars to be evaluated [21]. Wood chars contained microcrystalline particles with graphite-like planes organised turbostratically (the planes of carbon atoms are crumpled together rather than aligned parallel to each other). The d_{002} inter-layer spacing was ~0.38 nm and reduced with time of carbonisation. The micro-crystallite diameter L_a increased from 2 to 4 nm at soaking temperatures of 600 and 1,200 °C, respectively. The specific gravities increased from 1.35 to 1.65 as soaking temperatures increased from 400 to 1,200 °C, respectively. SEM examinations of the *Acacia* and *Eucalyptus* wood [22] under slow heating conditions revealed pyrolytic deposition of carbon in the resulting wood char structure which did not modify the wood microstructure. Rapidly heated wood developed cracks and voids during carbonisation between 800 and 1050 °C. Slow heating to maximum temperatures in the range of 800–1000 °C for extended periods resulted in sintering of wood fibres, compaction and densification.

Hirose et al. [23] manufactured liquid wood from hinoki (*Chamaecyparis obtusa* Endl.) powder mixed with a phenol compound and catalysed with sulphuric acid. Wood ceramics were formed from MDF impregnated with liquid wood, diluted with ethanol, followed by carbonisation in a vacuum furnace at 400, 500, 650 and 800 °C. The reduction in dimensions and loss of weight of the original MDF specimens increased with increasing carbonisation temperature. Density increased from about 700 to 800 kg m^{-3} and compressive strength rose from approximately 12 to 30 MPa. Volume resistivity fell from greater than 10^{11} to approximately 0.1 Ω cm, consistent with values for carbonised wood [20]. SEM images reveal a reduction in the dimensions of wood fibres in the MDF as carbonisation proceeds, but the porous structure of the MDF is essentially unchanged. The woody material is converted into soft amorphous carbon, whilst the phenol component is converted into hard glassy carbon. Wood ceramics are high in stiffness and corrosion resistance, and they are used for the production of electromagnetic shields.

The combination of wood fibres and phenolic resin binder was also employed by Celzard et al. [24] to manufacture carbonaceous monolithic materials. Wood fibres were mixed with 10% of powdered phenolic resin and pressed into boards before carbonisation in nitrogen up to 900 °C. The material contained random, compressed fibres which were almost pure carbon, and porosities ranged from 40 to 85%. The micropore and mesopore volumes were measured by nitrogen adsorption and mercury porosimetry, and found to be 0.2 and 0.02 cm^3 g^{-1}, respectively. Electrical conductivity (~10–60 S cm^{-1}) was measured using a four-probe method, and properties were suitable for applications as porous electrodes or light electromagnetic shields. The electrical and elastic properties of the carbonaceous monolith were successfully modelled using percolation theory (PT) and effective-medium theory (EMT).

Mechanically strong, chemically stable, ferromagnetic carbon electrodes were made by Ueda [25] from an oak (*Quercus* sp.) precursor. The oak wood was baked to form charcoal, and cobalt was introduced into the porous microstructure by impregnation with an aqueous solution of cobalt acetate such that the cobalt was 5% by weight of the charcoal. The charcoal/cobalt mix became ferromagnetic, confirmed by electron spin resonance spectrometry, after heating in a vacuum, and following acid extraction of the cobalt, the ferromagnetism was sustained. The ferromagnetism was strengthened by impregnation with hydrocarbons, and ferromagnetic electrodes were successfully manufactured based on the oak wood substrate.

Porous activated carbons are commercially significant in applications ranging from gas storage to odour absorption. Asakura et al. [26] produced fibrous activated carbons from softwood and hardwood fibres (species unspecified). Carbon fibres possess a high aspect ratio, and their efficiency as adsorbents is high compared with powdered or granulated carbons. The activation of conventional carbon fibres by oxidation involves the loss of a high proportion of their mass, and so the substitution of plant fibres as the precursor for activated carbon fibres (ACFs) is attractive. Wood fibres were pressed into plates and carbonised at 900 °C at a heating rate of 5 °C min^{-1} in a nitrogen gas environment. SEM images reveal that the hollow structure of the individual wood fibres was retained with features such as bordered pits still evident. Carbon yield was about 26% for softwood and hardwood fibres, and the samples were activated with carbon dioxide at 880 °C resulting in burn-off which was limited to levels of about 43 and 68% for softwoods and 40 and 70% for hardwoods. The pore characteristics of the ACFs were derived from nitrogen adsorption isotherms, and specific surface area, micropore volume and average pore size were calculated using Brunauer–Emmett–Teller (BET) analysis. The specific surface area of the softwood averaged 1,087 and 1,269 m^2 g^{-1} for 43 and 68% burn-offs, respectively, and the higher surface area with longer burn-off time was the result of more micropore development. For hardwoods, the specific surface area was 874 and 1,386 m^2 g^{-1} for 40 and 70% burn-offs, respectively. The adsorption of toluene and water vapour by these fibres was found to be comparable with commercial ACFs. In another study on ACFs, Okabe et al. [27] spun thin carbon fibres from waste wood-derived phenolic resin carbonised in nitrogen for 1 h at 1,000 °C. The BET-specific surface area increased from 13 m^2 g^{-1} before activation with steam to 1,048 m^2 g^{-1} afterwards, because of the increase in micropore volume.

Several recent studies have examined the molecular structure, nanostructure and microstructure of wood soot and carbonised wood. Arrais et al. [28] examined the soot deposits from domestic wood combustion, for example, from fireplaces, ovens and boilers. Graphitised carbonaceous particles are usually regarded as being of no commercial use, whereas wood ash may be used as fertiliser or for the saponification of fat triglycerides. However, the carbonaceous residues are a source of graphenic and aromatic substrates that could by chemical treatment produce polycondensed aromatic macromolecules and polycyclic aromatic hydrocarbons (PAHs) which find applications in surfactant chemistry, wetting additives, catalysis, membranes, dyes and inks and fluorescence markers. The article is complex and includes spectral analyses including SEM-EDX, XRD, Raman, FTIR, C-NMR (carbon nuclear magnetic resonance) and UV–VIS of carbonaceous flame combustion residues and describes the extraction and analysis of graphenic and aromatic derivatives. The carbonaceous residues were found to possess disordered structures similar to those of carbon black and glassy carbon.

Two articles by Ishimaru and co-workers examine the carbonisation process for wood, and in the first article [29], the initial steps in this process between 500 and 1,000 °C are determined by elemental analysis, FTIR, XPS and micro-Raman spectroscopy. The carbonisation of the wood cell wall of Japanese cedar (*Cryptomeria Japonica*) and of cotton cellulose fibre and lignin are compared. The degree of order of the carbonised wood microstructure is the lowest for cellulose and the highest for lignin. The cellulose content of wood and the carbon-to-oxygen ratio markedly influence ordering of the microstructure composed of crosslinked polyaromatic carbon stacks. In the second article [30], the Japanese cedar was carbonised at 700 and 1,800 °C and SEM, transmission electron microscopy (TEM) and micro-Raman spectroscopy were employed to analyse the inner planes of the wood cell walls. Figure 5 describes the location of ultra-thin TEM sections and the orientation of the carbonised wood for Raman analysis. The aim was to determine the structural changes caused by the conversion of the wood cell wall to carbonised wood. In Fig. 6 the wood cell wall is imaged by SEM before and after carbonisation at 700 °C. The well-defined cell wall layers in the original wood are replaced by a cellular structure composed of monolithic material. TEM images reveal 1–2 nm carbon crystallites homogeneously distributed in the cell wall following carbonisation at 700 °C. The crystal size increases to 3–8 nm after carbonisation at 1,800 °C. Raman spectroscopy identified sp^2-bonded carbon atoms with very little difference between structure at spot A (middle lamella) or spot B (secondary cell wall) identified in Fig. 5. At spot C, there was better ordering of carbon crystallites on the inner surface of cell walls. It is proposed that pyrolysis gases condense in the cell lumens during carbonisation resulting in ordered carbon crystallites. Hence, it is observed that the heterogeneous structure of wood is lost during the process of carbonisation.

A laminated carbon structure, designed to dissipate heat in a solar-powered satellite, was fabricated by hot pressing layers of carbonised Sugi wood (*Cryptomeria japonica*) and pure graphite [31]. The Sugi wood was carbonised at 700 °C in argon gas in an electric furnace. The carbonised wood (C) and graphite (G) were separately granulated in a vibration mill and three layer G/C/G composites were produced by hot-pressing at 700 °C with different proportions of C to G from 10 to 80%. The density, morphology and horizontal (H) and vertical (V) thermal conductivities of the laminated structures were measured, and Raman spectroscopy analysed the carbon structures before and after lamination. Anisotropy in thermal conductivity was improved by lamination with the highest H/V ratio at 10 wt% of carbonised wood. The quality of the C–G interface also affected conductivity. The microstructure of the graphite was highly ordered, whereas the carbonised wood was disordered/turbostratic.

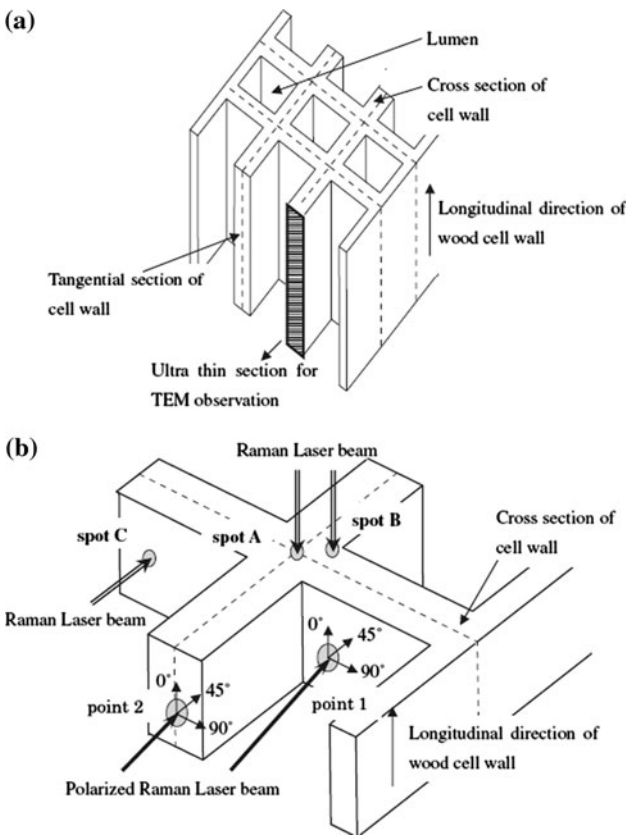

Fig. 5 Orientation of carbonised wood for **a** taking thin sections for TEM and **b** Raman spectroscopy [30]

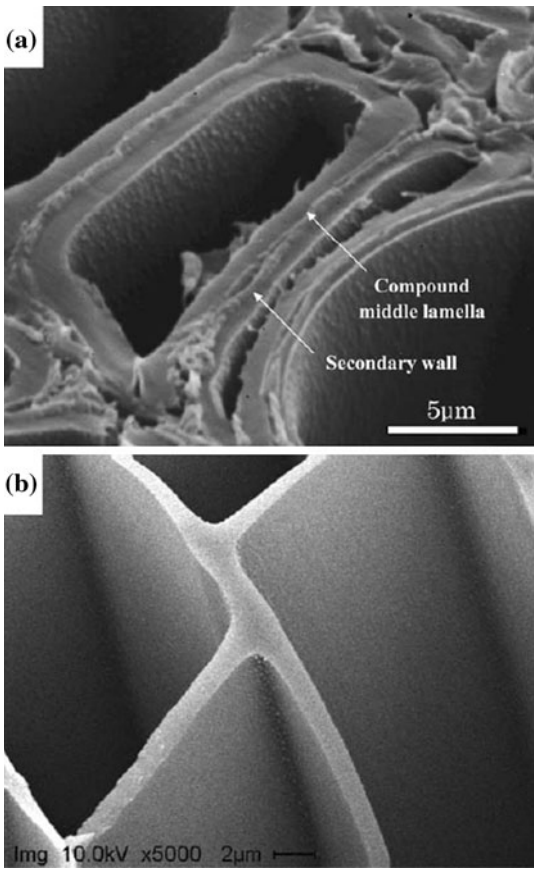

Fig. 6 SEM images for wood **a** before and **b** after carbonisation at 700 °C [30]

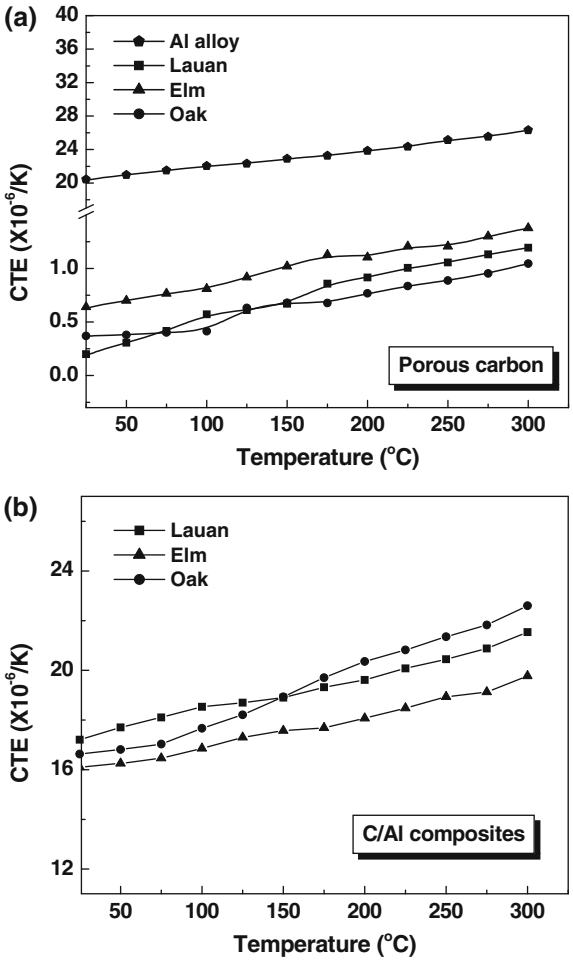

Fig. 7 Coefficient of thermal expansion as a function of temperature for **a** porous carbon and **b** composites [32]

Carbon composites based on wood templates

Fascinating developments in the manufacture of composite structures based on carbonised wood with the cellular cavities infiltrated with metal or ceramic are reviewed here. Wang et al. [32] pyrolysed lauan (*Shorea* sp.), elm (*Ulmus* sp.) and oak (*Quercus* sp.) wood for use as plant templates for infiltration by aluminium alloy. These species are all hardwoods with well-defined vessels which take up a large proportion of the wood volume. Carbonisation took place at 1,400 °C for 2 h in a vacuum. Aluminium alloy was injected into the cellular-carbonised structures at 720 °C under high pressure where it cooled to form an aluminium/wood composite. The size of the cell cavities determined the shape of aluminium fibres, but in oak not all cavities were filled probably because of the presence of membranes in the vessels called tyloses. The thermal expansion coefficients of the wood composites lay between those of the carbonised wood and the aluminium alloy alone (Fig. 7). The bending and compression strengths of the wood composites were significantly greater than the porous carbon (Fig. 8).

Several research groups have published studies on porous ceramic structures derived from carbonised wood substrates. Luo et al. [33] used beech wood (*Fagus* sp.) as a template for the fabrication of titanium nitride (TiN)/carbon composites using sol–gel processing and carbothermal reduction nitridation of TiO_2 composites in a nitrogen atmosphere (Eq. 3):

$$2TiO_2 + 4C + N_2 \rightarrow 2TiN + 4CO \quad (3)$$

Beech samples were shaped and dried, and titania sol was prepared from tetrabutyl titanate, acetylacetone and distilled water. Beech samples were placed in a vessel which was evacuated and titania sol was backfilled. The pressure in the vessel was raised, and it was left overnight following which the sol was gelled and dried at 130 °C. Carbonisation took place in a furnace at 800 °C in nitrogen resulting in a titania/charcoal composite. The proportion of TiO_2 was improved by repeating the process several times. Carbothermal reduction and nitridation at 1,400 °C

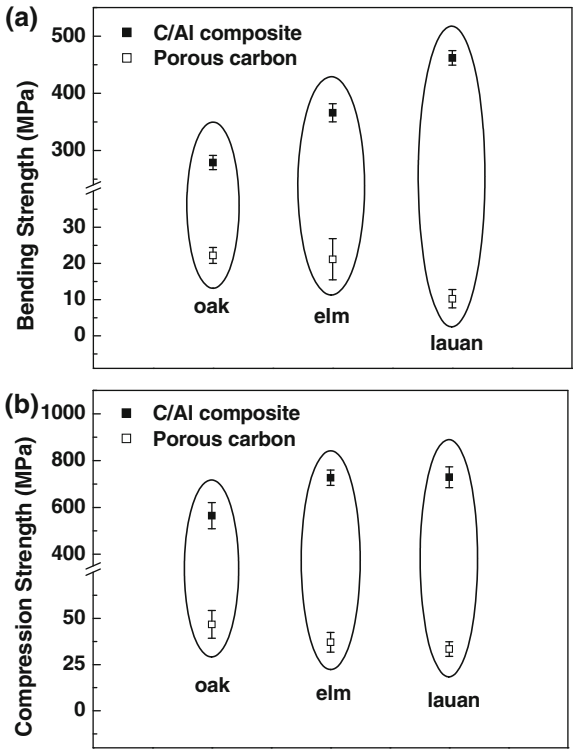

Fig. 8 **a** Bending strength and **b** compression strength of porous carbon and C/Al composites [32]

produced cubic TiN ceramic confirmed by XRD. The carbon was released by carbon monoxide evaporation and the biomorphic TiN closely resembled the original biocarbon template.

Porous TiN ceramics were also produced by Ohzawa et al. [34] who used pressure-pulsed chemical vapour infiltration of porous carbon substrates including cedar wood (species not specified). The wood was carbonised at 1,000 °C and subsequently infiltrated with a mixture of $TiCl_4$, N_2 (1%) and H_2 (10%) using a repeated pressure-pulse method. Electro-conductive porous ceramics were produced and resistivity depended on the composition of the TiN which was controlled by the ratio of gases in the chemical vapour infiltration process. Possible applications include rechargeable battery technology where active materials would fill the pores in the ceramic.

Varela-Feria et al. [35] infiltrated liquid silicon into pyrolysed beech wood (*Fagus* sp.). Pyrolysation took place at 1,000 °C in argon and infiltration with liquid Si was carried out at 1,450 °C under a vacuum. The resulting bio-silicon carbide was evaluated by electron backscattering diffraction. A reaction between the liquid silicon and the cell walls of the carbonised beech wood preform forms a solution from which micron-sized SiC grains are precipitated. Models for this reaction are proposed for large and narrow channels in the perform. Applications for the biomorphic SiC include heating elements, medical implants and high temperatures absorbers.

Finally, Sulistyo et al. [36] produced porous $SiC/SiO_2/C$ composites from carbonised wood infiltrated with SiO_2. Sugi wood (*Cryptomeria japonica*) was carbonised at 700 °C in nitrogen, and the carbonised wood was granulated and submerged in SiO_2 solution prepared by diluting ethylsilicate-40 with ethyl alcohol. The dried, infiltrated, carbonised wood was then compressed between graphite punches and sintered at temperatures ranging from 1,200 to 1,800 °C in a nitrogen atmosphere. The resulting material was analysed by XRD, Raman spectroscopy and XPS. Microstructure was observed by SEM and TEM with thin section produced by focussed ion beam etching (FIB). Electrical and thermal conductivities were also measured. Composition, crystal structure and electrical and thermal conductivities were all affected by the processing parameters. The high thermal conductivity of these ceramics would suit applications in solar power satellites.

Wood–cement composites

The majority of articles on wood–cement composites published in JMS emanate from the Commonwealth Scientific and Industrial Research Organisation (CSIRO) in Australia and the Building Research Establishment (BRE) in the UK.

Coutts and co-workers (CSIRO) produced a series of articles on wood fibre-reinforced cements (WFRCs) and plasters. The study was motivated by the low density, cost and embodied energy of wood fibre. In the first publication [37], Portland cement was chosen for the cement matrix, and two types of wood pulp (thermo-mechanical and kraft) were selected for evaluation as the fibre component. The effects of the proportion of wood fibre and the water-to-cement ratio on strength (three-point bending) and fracture energy of the composites were reported. The thermo-mechanical pulp was more suited to formulations with a low water-to-cement ratio. In a second article [38], Pinus radiata kraft pulp were soaked in water and disintegrated in a beater and combined with equal quantities of ordinary Portland cement and silica in a slurry/vacuum de-watering process followed by autoclaving. Samples were tested in three-point bending at 50% RH and 22 °C, and fracture topography was imaged by SEM. Failure occurred by fibre fracture and pull-out, and the interfacial bonding between fibre and cement matrix was significant. The effect of moisture on fracture mode was also evaluated [39]. The fracture surface of dry WFRCs contained broken fibres with fragments of matrix attached indicating a strong chemical bond, whereas the wet WFRCs exhibited fibre pull-out. Hydrogen bonds and/or hydroxide bridges were

postulated to control mechanical properties. In order to improve the wet strength of wood-fibre reinforced cements, curl was induced in the kraft pulp fibres [40] by processing in a planetary mixer. Wet inter-laminar bond strengths were improved by using curly fibres but modulus of rupture and fracture toughness were unchanged.

CSIRO studies on wood fibre-reinforced plaster of Paris (gypsum, β-hemihydrate) [41] employed either a high calcined gypsum-to-water ratio or slurry/vacuum dewatering which avoids clumping of the beaten *Pinus radiata* kraft fibre. In mechanical tests, the fracture toughness of the plaster was increased by more than a factor of 40 by addition of fibre, and flexural strength increased by a factor of two to three. A description of the microstructure of these composites [42] and the effect of casting pressure on mechanical properties [43] are also reported.

Fan and co-workers (BRE) published a trio of articles on the dimensional instability of cement bonded particleboards (CBPBs). Wood chips (species unspecified) were dissected from a CBPB and exposed to moist air at 35, 65 and 90% RH [44]. Changes in mass, length and thickness were measured as a function of time during an adsorption (35–90% RH) and desorption (90–35% RH) cycle, and changes were compared with raw wood chips and CBPB. Mass increase and dimensional changes on adsorption were in the order: raw wood chips > dissected chips > CBPB due to penetration of the cement liquid into cell lumens, cracks and fissures. A similar ranking order emerged under cyclic loading. Hysteresis lops were generated by plotting mass change versus relative humidity and the behaviour of dissected chips was similar to CBPB.

SEM and image analysis (IA) were employed [45] to characterise the structure of CBPB. As a result of mat formation in CBPB, the void distribution was concentrated in the board core. There was evidence of compression of wood chips in the direction of pressing of the boards, and the area occupied by cement paste in horizontal sections parallel to the plane of the board was greater than in vertical sections as a result of differential compression. Short, smooth chips were located at both the surface of the board and in the board core and longer and coarser chips were located elsewhere.

Image analysis was also employed in a third article [46] to determine the distribution, size, shape and area of occupied by the components of CBPB in vertical and horizontal sections. The equilibrium moisture content (EMC) of CBPB lay between those of the wood particles and the cement, and density profiles were determined by the distribution of cement paste and wood particles. Mass and dimensional changes in CBPBs were measured as a function of change in relative humidity. These changes were the results of the combined effects of moisture sorption and desorption (Fickian behaviour) or carbonation and degradation (non-Fickian behaviour). Good agreement was found between measured parameters and theoretical predictions.

Cheumani et al. [47] used proton low-field NMR relaxometry to evaluate the hydration of wood–cement composites. Commercial white Portland cement was combined with ground wood chips from *Eucalyptus saligna* and *Afzelia bipendensis* (collective name Doussie). Wood sawdust was added to dry cement with a wood-to-cement weight ratio of 0.2, and water was added to form composites with a water-to-cement ratio of 0.5. Two populations of water in the wood composites were monitored with NMR during the first 4 weeks of hydration, namely, gel and capillary moisture. Mainly unbound moisture migrated from the wood cell cavities to take part in the hydration of the cement, but some portion was retained as unbound or bound moisture. *E. saligna* was found to be more compatible with the process of cement hydration than *Afzelia bipendensis*. NMR relaxometry provided a clear insight into the hardening processes that occur in wood–cement composites.

Wood–polymer composites

The literature on cellulose–polymer composites is extensive, and so this review of JMS articles concentrates on WPCs containing solid wood, wood flour, wood fibre, wood powder or wood pulp. The role of the wood component in WPCs may be as reinforcement or filler depending on factors, such as chemical surface treatment of the wood component, and whether the matrix is a thermoplastic or a thermosetting polymer.

Munoz-Escalona et al. [48] impregnated six low-density tropical hardwoods with vinyl monomers and crosslinked them using a ^{60}Co source of radiation. The aim was to produce dense wood composites with properties equal to those of denser hardwoods. Whilst mechanical properties were improved, fracture surfaces revealed that impregnation was uneven, and properties did not match those of denser hardwoods. However, these composites may suit applications where wear resistance, dimensional stability and reduced anisotropy are required.

Wood flour prepared from trembling aspen (*Populus tremuloides*) was mixed with high-density polyethylene (HDPE) and compression moulded to form composites with different weight fractions of wood flour [49]. Different coupling agents, including silanes and polymethylene polyphenyl isocyanate (PMPPIC), were either applied as a coating to the fibre or mixed with the polymer to enhance surface adhesion at the wood flour to polymer interface. Tensile strength and stiffness were improved by the use of coupling agents, and PMPPIC was found to be the most

effective treatment. However, toughness in impact was reduced following the use of coupling agents.

Zhang et al. [50] produced HDPE matrix WPCs incorporating a maleic anhydride (MA) –HDPE coupling agent and pine softwood fibre (species unspecified). The mix ratio used in the compounding and extrusion process was HDPE:wood fibre:MA–HDPE:lubricant equal to 70:30:3:3. The aim of the study was to produce a foamed structure containing very small gas bubbles to increase impact strength and ductility and to reduce density. Rather than using environmentally negative chemical blowing agents, sc-CO_2 was substituted, and in order to understand the foaming process, the shear viscosity of the polymer/gas solution was measured using the extruder set-up illustrated in Fig. 9. Three sc-CO_2 contents of 1, 2 and 3% were selected at three die temperatures of 135, 140 and 145 °C, respectively. The Carreau–Yasuda model and the Arrhenius equation were employed to model the effects of temperature, pressure and sc-CO_2 on plasticisation of the mixture. The development of small and regular cells in the foamed structure favoured lower die temperatures which caused high pressure drop rates and shifted the position of the super-saturation point towards the die exit.

Sanadi et al. [51] developed a macroscopic pull-out test to measure the shear properties in the interphase region between wood and thermoplastic polymers where physical properties differ from the two main phases. The aim was to assess the effects of surface treatments and exposure to moisture on shear properties. Hardwood birch (*Betula* sp.) dowels were acetylated and treated with an anionic emulsion of maleated polypropylene (MAPP) or an emulsion copolymer of ethylene and acrylic acid (EPA). A cylinder of low molecular weight polyethylene was melted around the dowel, and pull-out tests were conducted to measure debonding force versus embedded length. Shear strength was calculated as a function of embedded length, and the work of fracture in the interphase region was estimated. MAPP- or EPA-treated dowels improved shear strength, and the experimental technique was recommended for the evaluation of wood thermoplastic combinations for composites based on recycled feedstock.

The measurement of interfacial shear strength was also included in a article by Kazayawoko et al. [52], which evaluated composites composed of bleached kraft pulp (BKP) or unbleached thermo-mechanical pulp in a polypropylene (PP) matrix. MAPP was used as a coupling agent, and the wood species were balsam poplar (*Populus balsamifera* L.) and red oak (*Quercus rubra* L.). Wood fibre/PP/MAPP combinations are frequently used for manufacturing composites by extrusion or injection moulding. Maleic anhydride and other chemical treatments were also assessed. The chemical bonds at the wood fibre to PP interface were identified with FTIR, and inverse gas chromatography (IGC) was employed to estimate the work of adhesion. The average interfacial shear strength between wood veneer and PP was measured in a pull-out test on lengths of veneer-embedded in PP. FTIR confirmed the formation of ester linkages by an esterification reaction between BKP fibres and anhydride groups of MAPP, but no ester linkages were formed with TMP fibres. IGC results suggest that the thermodynamic work of adhesion is not enhanced by MAPP treatment and that other mechanisms are responsible. Interfacial shear strengths ($\sim$2 MPa) were improved by roughening of the wood veneer and by treatment with MAPP. The tensile and flexural strengths were significantly increased by MAPP treatment as a result of better wetting at the fibre to matrix interface. Confocal microscopy confirmed an even dispersion of wood fibres in the PP matrix, but injected moulded composites exhibited orientation in the flow direction.

In a second article on PP matrix composites [53], the fibre content was southern pine (*Pinus palustris*) wood flour, esterified with octanoyl chloride (OC) in either chloroform or dimethylformide (DMF). The OC reacts with surface hydroxyl groups and improves reactivity with the PP matrix. A second approach was to add MAPP to the

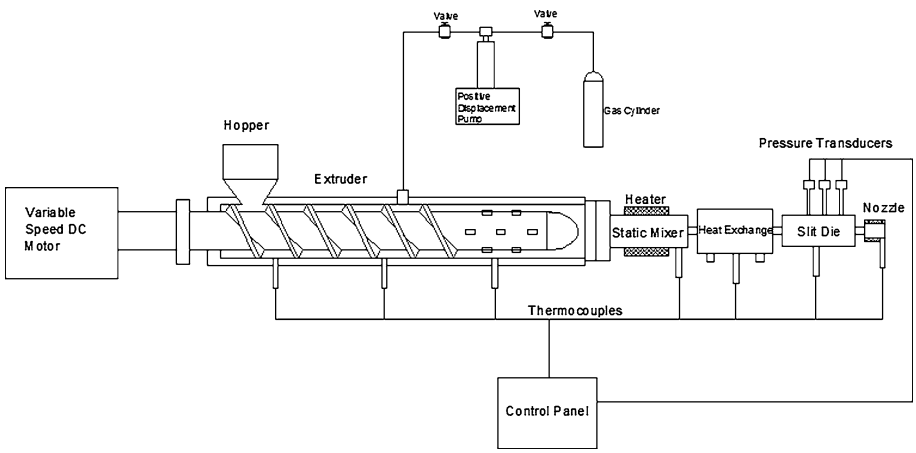

Fig. 9 Schematic of the extruder set-up for the measurement of WPC/supercritical CO_2 solution viscosities [50]

PP to promote the formation of ester linkages with the wood powder. The mechanical performance of the composites and their moisture uptake were compared. Both the OC and MAPP treatments reduced moisture uptake compared with the unmodified composite, but OC treatment reduced the flexural strength and modulus of elasticity. In contrast, loadings of MAPP up to 5 wt% increased mechanical properties by producing MAPP/PP entanglements. It should be noted that whilst wood flour is commonly used as a filler, the flexural modulus of PP is increased by wood flour additions and hence the wood flour acts as a reinforcement as well as a filler.

A further article [54] on the properties of PP/wood pulp composites modified with MAPP examined the distribution of fibre lengths and alignment following extrusion. Fibre length was determined with a fibre quality analyser and X-ray computed tomography was used to produce a 3-D image of microstructure. Most fibres were 0.2–1.0 mm in length and, as the fibre content increased, there was more alignment along the specimen axis due to compression and the geometry of the extruder die.

Continuing the theme, PP/MAPP matrix composites were manufactured by extrusion and injection moulding [55] with the addition of wood fibre and olive mill sludge (OMS) which is a major waste product in Mediterranean countries much of which goes to landfill. Wood particles were supplied from a particleboard plant and comprised equal quantities of pine (*Pinus nigra* Arnold var. *pallasiana*) and beech (*Fagus orientalis* Lipsky). Wood flour content range from 0 to 40 wt% and dried OMS flour from 0 to 40 wt%. PP content was 57 or 60 wt% and MAPP was 0 or 3 wt%. OMS residues proved to be a suitable reinforcement for WPCs and the OMS flour reduced moisture uptake. However, flexural properties declined with OMS content and MAPP addition had little effect on this decline. A ratio of 40 wt% OMS to 60 wt% PP appears to offer the optimum properties.

A final JMS article [56] on PP/MAPP/wood flour composites assessed the effect of the addition of carbon nanotubes (CNTs) on thermal properties and flammability. Wood flour was composed of poplar sawdust (*Populus* sp.) and CNTs were 20–30 nm in diameter and 5–10 μm in length. Hydroxylated nanotubes were also prepared in-house. Wood flour content was maintained at 40 wt% and MAPP at 10 wt%. CNT content (as received or hydroxylated) was varied between 0.5, 1.0 and 2.0 wt%. The constituents were blended at 180 °C in a mixer and pressed at 15 MPa at the same temperature. MAPP addition had a marked effect on improving tensile strength of the resulting composites by a factor of approximately two, and nanotube addition at the 0.5 wt% level resulted in the optimum tensile properties with the highest elongation at break. TGA revealed an initial degradation temperature of 272 °C for the PP/wood flour base composite. MAPP and CNT additions extended the range of thermal stability. In cone calorimeter tests, the peak heat release rate was reduced by CNT additions as a result of a thermal barrier effect and radical-trapping effect.

Tannin and wood flour composites were investigated by Yano et al., where the aim was to replace formaldehyde-containing thermosetting polymers with tannin [57]. Tannin was extracted from the bark of radiata pine (*Pinus radiata* D. Don) by grinding and extraction with water at 100 °C. Wood flour (radiata pine) with particle size of <0.16 mm was combined with the tannin in the ratio of 1:1 and hot-pressed in a die at 190 °C and 100 MPa. An alternative process combined a tannin solution with wood flour and formalin followed by freeze drying before hot pressing to improve tannin impregnation. A comparison was made with conventional Bakelite–wood flour composites. Mechanical properties of the wood flour–tannin and wood flour–bakelite composites were similar and, following boiling tests in water, environmental stability was found to be similar. High-strength-moulded composites could be manufactured without formaldehyde probably because of autocondensation of the tannin.

Wood flour (pine) was combined with a starch–cellulose acetate blend, blended in a twin screw extruder and injection moulded [58]. The processability of the resulting biodegradable composite was improved by the addition of glycerol. The shear viscosities of the blended constituents and the injection-moulded melts were studied by capillary rheometry, and quasi-Newtonian behaviour was observed. Optimum mechanical properties were achieved with a wood fibre content of 50 wt%, but the wood fibre acted as a filler with an adverse effect on toughness.

Gindl and Jeronimidis [59] impregnated beech sulphite pulp fibres with melamine–formaldehyde (MF) resin with the aim of producing dimensionally stable wood fibre composites with low moisture uptake. Impregnation took place either by employing a vacuum technique or at atmospheric pressure by soaking. Composite sheets were hot pressed at 120 °C at 20 MPa for 10 min. SEM images demonstrated that MF was compatible with the pulp fibres and boiling in water for 2 h only reduced Young's modulus to 60% and tensile strength to 70% of its initial value.

The manufacture of WPCs from plastic and wood wastes offers an environmentally acceptable solution for the reduction of two major sources of waste. Wood flour (species unspecified) was combined with HDPE to form flat plates by Huang et al. [60], and flexural strength and modulus were assessed in three-point bending, and fracture toughness by single edge notch bending (SENB). Specimens were also soaked in water for up to 30 days whereafter the initial flexural modulus ($\sim$2.7 GPa) was reduced by $\sim$25% and the initial flexural strength ($\sim$26 MPa) by

~14%. The critical strain energy release rate G_{IC} was reduced from 4,500 to ~2,600 J m^{-2} at a moisture content of 2%.

Laborie and Frazier [61] assessed the interaction between yellow poplar (*Lirodendron tulipifera*) wood powder and PF resin by nuclear magnetic resonance (^{13}C NMR) studies. The wood fibre was mixed with PF and cured in an oil bath at 150 °C for 15 min. NMR revealed no intermolecular interaction between the wood protons and the resin nuclei in the wood composite. The PF hydroxyl-bearing carbons experienced a downshift signifying secondary interactions between the PF and the wood.

Another approach to recycling wood waste is to manufacture materials from wood powder by steam compression without the addition of a matrix phase. Miki et al. [62] crushed mixed Japanese and cypress and cedar chips in a ratio of 1:1 to form wood powder which was pressed at a pressure of 36.5 MPa in the temperature range 100–170 °C for 30 min. The density, bending strength and modulus of elasticity and Charpy work of fracture were measured, and dynamic mechanical thermal analysis (DMTA) measured viscoelastic characteristics in the dry and wet states to assess thermoplastic qualities. All static properties improved with increasing steaming temperature, except for the work of fracture which peaked at 140 °C. The peak static strength (~75 MPa) and peak flexural modulus (~8 GPa) are very respectable values for a random wood powder composite. Bonding of the wood powder is thought to occur by auto-condensation of the molecular components of wood, including hemicelluloses and lignin, together with mechanical interlocking. Wetting the material (Fig. 10) results in an increase in loss tangent in the range 30–90 °C through interaction with the lignin content, but successive wetting and drying cause a progressive hardening of the material. It is proposed that items can be shaped by steam processing and subsequently hardened by drying.

Friction grinding was employed by Bulota et al. [63] to produce microfibrillated cellulose (MFC) from birch (*Betula* sp.) wood pulp. Composites were prepared with a polymer matrix consisting of either poly(vinyl) alcohol (PVA) or a copolymer of PVA and MMA. Composite films were prepared by dissolving the polymer in water, adding the MFC gel and casting the MFC dispersion onto a glass plate, with or without degassing. The aim of the article was to assess the influence of preparation technique on mechanical properties and to compare properties with predictions from the Rule of Mixtures, the Halpin-Tsai equation, a modified rule of mixtures where the matrix and fibre modulus are raised to a power of 1/5 and a percolation model. Tensile strengths lay in the range 40–70 MPa, and tensile modulus in the range 1.4–4.9 GPa depending on the preparation method, fibre loading and relative humidity.

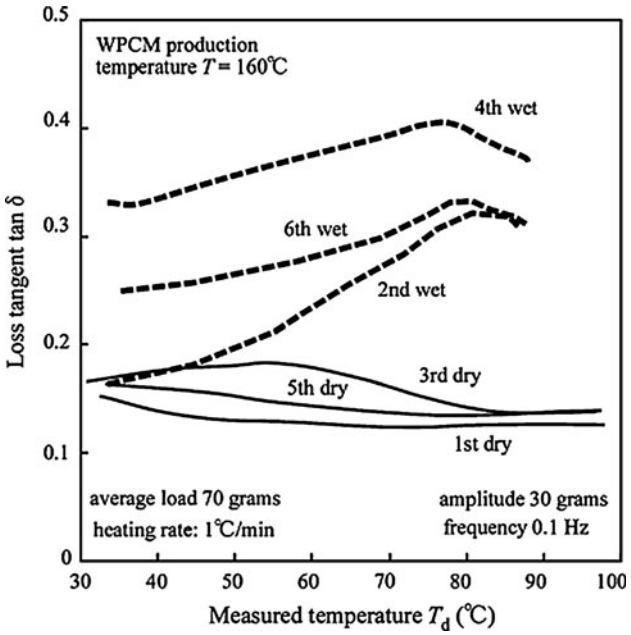

Fig. 10 Effect of cyclic wetting and drying on dynamic loss tangent as a function of temperature for steam compressed wood powder [62]

The experimental results for tensile modulus plotted versus MFC content corresponded with the predictions of the modified rule of mixtures and percolation theory.

Whilst research on cellulose nanofibres is strictly outside the scope of this JMS review on wood, readers may wish to pursue the latest developments in the preparation and characterisation of cellulose nanofibres with elastic moduli being predicted to be as high as 220 GPa and with potential for the reinforcement of polymer composites. For example, Qua et al. [64] prepared cellulose nanofibres from flax or microcrystalline cellulose by high-energy ball milling, acid hydrolysis and ultrasound or by high-pressure homogenisation in a microfluidiser. The microstructure of nanocellulose was imaged by SEM and TEM, and nanofibre diameters were of the order of 8 nm. Aspect ratios were measured by dynamic light scattering; chemical constitution was analysed by FTIR and thermal stability by TGA. Acid hydrolysis was found to cause esterification of hydroxyl groups on the cellulose, but reduced overall crystallinity. Repeated passes through the microfluidiser increased the crystallinity index and thermal stability. A very comprehensive review of cellulose nanofibres and nanocomposites is provided by Eichhorn et al. [65].

Conclusions

The second part of this anniversary review has revealed the extraordinary versatility of wood and the plethora of applications for this natural resource. In many ways, wood

possesses key advantages in terms of wide availability in a range of densities, renewability, machinability, low cost, and the advantage of strong aesthetic appeal. In other respects, the disadvantages of dimensional instability when exposed to moisture and heat, flammability, time-dependent mechanical properties and susceptibility to biodegradation provide technical challenges for users of wood. A broad view of the JMS literature has identified advances that have addressed these challenges. It is clear that, in recent years, the routine availability of state-of-the-art techniques for chemical and thermal analyses, such as XPS, NMR and Raman spectroscopy, have significantly improved our understanding of processes, such as interfacial bonding, hydration, carbonisation and wood modification. There is no doubt that, in the years to come, wood will continue to be the subject of cutting-edge research whether as a source of microcrystalline and nanofibrous cellulose for composite materials or as the basis for improved structural materials.

References

1. Ansell MP (2011) J Mater Sci 46:7357. doi:10.1007/s10853-011-5856-2
2. Hill CAS (2006) Wood modification—chemical, thermal and other processes. Wiley, Chichester
3. Sugiyama M, Obataya E, Norimoto M (1998) J Mater Sci 33:3505. doi:10.1023/A:1004678506822
4. Sugiyama M, Norimoto M (2003) J Mater Sci 38:4551. doi:10.1023/A:1027341804093
5. Obataya E, Shibutani S (2005) J Mater Sci 40:4113. doi:10.1007/s10853-005-0641-8
6. Ishikura Y (2011) J Mater Sci 46:3785. doi:10.1007/s10853-011-5292-3
7. Goswami L, Eder M, Gierlinger N, Burgert I (2008) J Mater Sci 43:1286. doi:10.1007/s10853-007-2162-0
8. Garcia RA, Riedl B, Cloutier A (2008) J Mater Sci 43:5037. doi:10.1007/s10853-008-2596-z
9. Tomak ED, Hughes M, Yildiz UC, Viitanen H (2011) J Mater Sci 46:598. doi:10.1007/s10853-010-4859-8
10. Tomak ED, Viitanen H, Yildiz UC, Hughes M (2011) J Mater Sci 46:608. doi:10.1007/s10853-010-4860-2
11. Sinn G, Reiterer A, Stanzl-Tschegg SE (2001) J Mater Sci 36:4673. doi:10.1023/A:1017954300015
12. Sinn G, Mayer H, Stanzl-Tschegg S (2005) J Mater Sci 40:4325. doi:10.1007/s10853-005-1995-7
13. Rautkari L, Laine K, Laflin N, Hughes M (2011) J Mater Sci 46:4780. doi:10.1007/s10853-011-5388-9
14. Kocaefe D, Chaudhry B, Poncsak S, Bouazara M, Pichette A (2007) J Mater Sci 42:854. doi:10.1007/s10853-006-0054-3
15. Kocaefe D, Poncsak S, Tang J, Bouazara M (2010) J Mater Sci 45:681. doi:10.1007/s10853-009-3985-7
16. Li P, Oda J (2007) J Mater Sci 42:8544. doi:10.1007/s10853-007-1781-9
17. Eastman SA, Lesser AJ, McCarthy TJ (2009) J Mater Sci 44:1275. doi:10.1007/s10853-008-3224-7
18. Tsioptsias C, Panayiotou C (2011) J Mater Sci 46:5406. doi:10.1007/s10853-011-5480-1
19. Sun Q, Yu H, Liu Y, Li J, Cui Y, Lu Y (2010) J Mater Sci 45:6661. doi:10.1007/s10853-010-4758-z
20. Kumar M, Gupta RC (1993) J Mater Sci 28:440. doi:10.1007/BF00357821
21. Kumar M, Gupta RC, Sharma T (1993) J Mater Sci 28:805. doi:10.1007/BF01151261
22. Kumar M, Gupta RC (1995) J Mater Sci 30:544. doi:10.1007/BF00354423
23. Hirose T, Fan TX, Okabe T, Yoshimura M (2001) J Mater Sci 36:4145. doi:10.1023/A:1017952502431
24. Celzard A, Treusch O, Marêché JF, Wegener G (2005) J Mater Sci 40:63. doi:10.1007/s10853-005-5688-z
25. Ueda H (2001) J Mater Sci 36:5955. doi:10.1023/A:1012945230587
26. Asakura R, Morita M, Maruyama K, Hatori H, Yamada Y (2004) J Mater Sci 39:201. doi:10.1023/B:JMSC.0000007745.62879.74
27. Okabe K, Yao T, Shiraishi N, Oya A (2005) J Mater Sci 40:3847. doi:10.1007/s10853-005-2561-z
28. Arrais A, Diana E, Boccaleri E (2006) J Mater Sci 41:6035. doi:10.1007/s10853-006-0511-z
29. Ishimaru K, Hata T, Bronsveld P, Meier D, Imamura Y (2007) J Mater Sci 42:122. doi:10.1007/s10853-006-1042-3
30. Ishimaru K, Hata T, Bronsveld P, Imamura Y (2007) J Mater Sci 42:2662. doi:10.1007/s10853-006-1361-4
31. Sulistyo J, Hata T, Fujisawa M, Hashimoto K, Imamura Y, Kawasaki T (2009) J Mater Sci 44:734. doi:10.1007/s10853-008-3159-z
32. Wang T-C, Fan T-X, Zhang D, Zhang G-D (2006) J Mater Sci 41:6095. doi:10.1007/s10853-006-0622-6
33. Luo M, Gao J, Zhang X, Hou G, Yang J, Ouyang D, Wang H, Jin Z (2007) J Mater Sci 42:3761. doi:10.1007/s10853-006-0425-9
34. Ohzawa Y, Cheng X, Achiha T, Nakajima T, Groult H (2008) J Mater Sci 43:2812. doi:10.1007/s10853-008-2537-x
35. Varela-Feria FM, Ramírez-Rico J, de Arellano-López DA, Martínez-Fernández Singh M (2008) J Mater Sci 43:933. doi:10.1007/s10853-007-2207-4
36. Sulistyo J, Hata T, Kitagawa H, Bronsveld P, Fujisawa M, Hashimoto K, Imamura Y (2010) J Mater Sci 45:1107. doi:10.1007/s10853-009-4053-z
37. Campbell MD, Coutts RSP (1980) J Mater Sci 15:1962. doi:10.1007/BF00550621
38. Coutts RSP, Kightly P (1982) J Mater Sci 17:1801. doi:10.1007/BF00540809
39. Coutts RSP, Kightly P (1984) J Mater Sci 19:3355. doi:10.1007/BF00549827
40. Michell AJ, Freischmidt G (1990) J Mater Sci 25:5225. doi:10.1007/BF00580155
41. Coutts RSP (1986) J Mater Sci 21:2959. doi:10.1007/BF00551516
42. Coutts RSP, Ward JV (1987) J Mater Sci Letts 6:562
43. Coutts RSP, Warden PG (1988) J Mater Sci Letts 7:918. doi:10.1007/BF00720729
44. Fan MZ, Dinwoodie JM, Bonfield PW, Breese MC (1999) J Mater Sci 34:1729. doi:10.1023/A:1004590621247
45. Fan MZ, Bonfield PW, Dinwoodie JM, Breese MC (2000) J Mater Sci 35:6213. doi:10.1023/A:1026733313070
46. Fan MZ, Bonfield PW, Dinwoodie JM (2006) J Mater Sci 41:5666. doi:10.1007/s10853-006-0286-2
47. Cheumani YAM, Ndikontar M, De Jéso B, Sèbe G (2011) J Mater Sci 46:1167. doi:10.1007/s10853-010-4888-3
48. Munoz-Escalona a, Bolsaitis P, Viela JE (1976) J Mater Sci 11:1711. doi:10.1007/BF00737527
49. Raj RG, Kokta BV, Daneault C (1990) J Mater Sci 25:1851. doi:10.1007/BF01045396
50. Zhang J, Rizvi G, Park CB, Hasan MM (2011) J Mater Sci 46:3777. doi:10.1007/s10853-011-5291-4

51. Sanadi AR, Rowell RM, Young RA (1993) J Mater Sci 28:6347. doi:10.1007/BF01352195
52. Kazayawoko M, Balatinecz JJ, Matuana LM (1999) J Mater Sci 34:6189. doi:10.1023/A:1004790409158
53. Zhang Y, Toghiani H, Zhang J, Xue Y, Pittman CU Jr (2009) J Mater Sci 44:2143. doi:10.1007/s10853-009-3295-0
54. Awal A, Ghosh Sain M (2009) J Mater Sci 44:2876. doi:10.1007/s10853-009-3380-4
55. Ayrilmis N, Buyuksari U (2010) J Mater Sci 45:1336. doi:10.1007/s10853-009-4087-2
56. Fu S, Song P, Yang H, Jin Y, Lu F, Ye J, Wu Q (2010) J Mater Sci 45:3520. doi:10.1007/s10853-010-4394-7
57. Yano HJ, Collins PJ, Yazaki Y (2001) J Mater Sci 36:1939. doi:10.1023/A:1017597924514
58. Cunha AM, Liu ZQ, Feng Y, Yi X-S, Bernardo CA (2001) J Mater Sci 36:4903. doi:10.1023/A:1011836220064
59. Gindl W, Jeronimidis G (2004) J Mater Sci 39:3245. doi:10.1023/B:JMSC.0000025870.09117.f6
60. Huang S-H, Cortes P, Cantwell WJ (2006) J Mater Sci 41:5386. doi:10.1007/s10853-006-0377-0
61. Laborie M-P, Frazier CE (2006) J Mater Sci 41:6001. doi:10.1007/s10853-006-0497-6
62. Miki T, Sugimoto H, Kanayama K (2007) J Mater Sci 42:7913. doi:10.1007/s10853-007-1723-6
63. Bulota M, Jääskeläinen AS, Paltakari J, Hughes M (2011) J Mater Sci 46:3387. doi:10.1007/s10853-010-5227-4
64. Qua EH, Hornsby PR, Sharma HSS, Lyons G (2011) J Mater Sci 46:6029. doi:10.1007/s10853-011-5565-x
65. Eichhorn SJ, Dufresne A, Aranguren M, Marcovich NE, Capadona JR, Rowan SJ, Weder C, Thielemans W, Roman M, Renneckar S, Gindl W, Veigel S, Keckes J, Yano H, Abe K, Nogi M, Nakagaito AN, Mangalam A, Simonsen J, Benight AS, Bismarck A, Berglund LA, Peijs T (2010) J Mater Sci 45:1. doi:10.1007/s10853-009-3874-0